REPORT DOCUMENTATION PAGE

AFRL-SR-AR-TR-05-

0431

1. REPORT DATE *(DD-MM-YYYY)*	2. REPORT TYPE	3. DATES COVERED *(From - To)*
14-09-2005	Final	06/14/02 - 12/14/04

4. TITLE AND SUBTITLE

Identification of the Factors Governing the Origin & Propagation of Corrosion Failure of Organically Coated Aluminum Aerospace Alloys

5a. CONTRACT NUMBER

5b. GRANT NUMBER
F49620-02-1-0301

5c. PROGRAM ELEMENT NUMBER
N/A

6. AUTHOR(S)
John R. Scully and Daryl A. Little

5d. PROJECT NUMBER
N/A

5e. TASK NUMBER

5f. WORK UNIT NUMBER
N/A

7. PERFORMING ORGANIZATION NAME(S) AND ADDRESS(ES)

University of Virginia
Office of Sponsored Programs
P. O. Box 400195
Charlottesville, VA 22904-4195 NL

8. PERFORMING ORGANIZATION REPORT NUMBER
UVA/116700-101-GG10444-31340

9. SPONSORING / MONITORING AGENCY NAME(S) AND ADDRESS(ES)
Air Force Office of Scientific Research
4015 Wilson Blvd., Arlington, VA 22203

10. SPONSOR/MONITOR'S ACRONYM(S)
N/A

11. SPONSOR/MONITOR'S REPORT NUMBER(S)
N/A

12. DISTRIBUTION / AVAILABILITY STATEMENT
Approved for public release, distribution unlimited.

13. SUPPLEMENTARY NOTES
N/A

14. ABSTRACT The effect of pretreatment and alloy microstructure on the rate of scribe-creep caused by under-paint corrosion on AA2024 was examined. Scribe-creep experiments were conducted on epoxy polyamide coated AA2024-T3 in 80% relative humidity at 25°C, 40°C, and 50°C with an intentional scratch through the organic coating into the substrate. Scribe-creep was enhanced by test temperature regardless of surface pretreatment with activation energy of 30-40 kJ/mol, as well as by artificial aging of the alloy and certain alloy surface pretreatments before the coating was applied. Scribe creep rates were accelerated at all temperatures by pretreatments that increased the surface copper coverage or left a high capacity for Cu-replating such as in the form of Cu-containing intermetallic compounds. Scribe creep was mitigated by pretreatments such as NaOH + HNO_3 as well as by chromate, molybdate and cerium acetate inhibitors that minimized Cu replating. Instrumented arrays were used to develop a galvanic corrosion model of scribe creep propagation that could account for many of the material, pretreatment and inhibitor effects seen on scribe creep propagation.

15. SUBJECT TERMS
alloy microstructure, scibe-creep experiments

16. SECURITY CLASSIFICATION OF:			17. LIMITATION OF ABSTRACT	18. NUMBER OF PAGES	19a. NAME OF RESPONSIBLE PERSON
a. REPORT	b. ABSTRACT	c. THIS PAGE			Scully, J. R.
Unclassified	Unclassified	Unclassified	UL	25	19b. TELEPHONE NUMBER *(include area code)* 434-982-5786

UNIVERSITY of VIRGINIA
ENGINEERING

POST AWARD ADMINISTRATION

September 13, 2005

Air Force Office of Scientific Research
Attn: Major Jennifer Gresham Ph.D.
4015 Wilson Blvd.
Arlington, Virginia 22203

SUBJECT: Final Technical Report on Grant Number F49620-02-1-0301
(UVA: 116700-101-GG10444-31340)

Dear Major Gresham,

Enclosed is the Final Technical Report under the direction of Dr. J. R. Scully on Grant Number F49620-02-1-0301. The project is entitled "Identification of the Factors Governing the Origin and Propagation of Corrosion Failure of Organically Coated Aluminum Aerospace Alloys" for the period June 14, 2002 through December 14, 2004. If you have any questions, you may contact Dr. Scully by e-mail at jrs8d@virginia.edu or 434-982-5786. We appreciate your support on this project.

Sincerely,

Sherry Fitzgerald
Administrative Assistant

Enclosure: Final Technical Report

Cc: Air Force Office of Scientific Research
Attn: Ms. Mary A. Moore
4015 Wilson Blvd.
Arlington, Virginia 22203-1954

Office of Naval Research
Atlanta Regional Office
100 Alabama Street, S.W., Suite 4R15
Atlanta, Georgia 30303-3104

Dr. J. R. Scully, MSE
Ms. Kristen Sellers, OSP
Ms. Faye B. Cline, SEAS

School of Engineering and Applied Science • 159 Engineer's Way • P.O. Box 400258 • Charlottesville, VA 22904-4258
Phone: 434-924-3931 • Fax: 434-924-6270

A Final Technical Report on AFOSR project
116700-101-GG10444-31340 (GRANT #F49620-02-1-0301)
Reporting Date 9/14/05

"Identification of the Factors Governing the Origin & Propagation of Corrosion Failure of Organically Coated Aluminum Aerospace Alloys"

Submitted by:

John R. Scully, Principle Investigator
Daryl Little, Ph.D. Candidate

The Center for Electrochemical Science and Engineering
Department of Materials Science
University of Virginia
Charlottesville, VA 22904-0745

Submitted to:

Major Jennifer Gresham Ph.D.
AFOSR
4015 Wilson Blvd.
Arlington VA, 22203

EXECUTIVE SUMMARY

Under-paint corrosion grows on metal surfaces under a coating. It can lead to pitting and intergranular corrosion under the paint which can act as a stress riser for stress corrosion cracking or fatigue. This study seeks to examine the effect of pretreatment and alloy microstructure on the rate of scribe-creep caused by under-paint corrosion on AA2024 in the T3 temper and when aged beyond it (T3 + 3 hrs @ 190°C, T3 + 12 hrs @ 190°C, T3 + 30 hrs @ 190°C, and T3 + 240 hrs @ 190°C). It is well known from literature that the Cu and Fe containing microstructure of aluminum alloys leads to the formation of galvanic cells between intermetallic compounds or replated Cu and the aluminum rich matrix and Cu-replating. Intermetallic compounds (IMCs) can serve as local anodic and cathodic sites as well as sources for Cu-replating. Additionally, Cu-replating may originate from the matrix. Literature has shown that the composition of the aluminum alloy, particularly Cu and Fe content, has a direct and dominant effect on the growth rate of filiform corrosion and scribe-creep process associated with under-paint corrosion. However, it is unclear whether the detrimental action of Cu and Fe in filiform corrosion occurs as a result of their presence in Al-Cu and Al-Cu-Fe intermetallic compounds or due to Cu-replating. Moreover, it is unknown whether anodic intermetallic compounds, cathodic IMCs, or some combination are required for initiation and propagation of under-paint corrosion. If the factors controlling scribe creep initiation and propagation were better understood then materials, coating, and finishing procedures to mitigate this form of corrosion could be proposed.

The effects of surface pretreatment and alloy aging that control the amount of surface copper and alter intermetallic compound distributions on the rate of scribe-creep caused by under-paint corrosion on coated AA2024-T3 were investigated. The effects of alloy aging on the rate of scribe-creep caused by under-paint corrosion on coated AA2024-T3 was also investigated. Scribe-creep experiments were conducted on epoxy polyamide coated (average coating thickness ~10 μm) AA2024-T3 in 80% relative humidity at 25°C, 40°C, and 50°C with an intentional scratch through the coating into the substrate. Scribe-creep was observed to be enhanced by exposure test temperature regardless of surface pretreatment with activation energy of 30-40 kJ/mol, as well as by artificial aging and surface pretreatments. Scribe-creep rate was accelerated at all temperatures by pretreatments that increased the

concentration of surface copper or left a high capacity for Cu-replating such as in the form of Cu-containing intermetallic compounds. Cyclic voltammetry tests conducted qualitatively compared the amount of copper on the surface after the various pretreatments performed on AA2024-T3. NaOH etching particularly increased the amount of replated Cu at the coated metal interface compared to an as-received condition and a NaOH etch followed by a HNO_3 deoxidation. The length, *l*, of the scribe-creep after a given time period was proportional to the test temperature through an Arrhenius type relationship and as a function of time as shown by Equation [1]. Scribe-creep rates decreased with time as "x" was typically less than one.

$$l = \mathrm{kt}^{x} = \mathrm{k}_{o} t^{x} \exp^{\left(-E/RT\right)} \qquad [1]$$

Experiments show that the Cu content of the alloy and pretreatment strongly influence scribe creep. The pre-exponential term, k, was greatest for the NaOH treatment followed by the as-received condition and the NaOH + HNO_3 pretreatment had the lowest k value. The effect of each surface pretreatment to enhance or retard scribe-creep was traced either to the initial level of Cu-replating prior to coating or to its ability to supply Cu for replating in the scribe-creep filament wake. When Cu was eliminated as an alloying element, or when surface Cu was minimized at the coating-metal interface by HNO_3 deoxidation pretreatment, scribe-creep corrosion rates were lowered. It should be noted that the effect of pretreatment was not traceable to coating adhesion. It was rationalized to occur as a result of a decrease in the cathodic oxygen reduction reaction rate, which supports anodic undercutting at the head of the corrosion front. NaOH pretreated specimens have improved adhesion but despite this the rate of scribe-creep was increased.

The accepted mechanism of scribe-creep in Al-based alloys is anodic undercutting.[1] In this mechanism, the scribe-creep will be proportional to the rate of the anodic dissolution process at the head. This, in turn, is proportional to the galvanic corrosion rate. Hence, it was desired to understand the galvanic corrosion process between the cathodic tail and the anodic head. The cathodic reaction which occurs on the Cu rich sites (replated and IMCs) is the oxygen reduction reaction. Cu-replating was found to enhance the rate of cathodic electron transfer reactions, which supports the galvanic corrosion process between scribe-creep head and tail.

Although some Cu-replating occurs in the wake of the filament head the main cathode is at the original defect (scratch). Literature results and experiments in this study supported the notion that the location of the primary cathode was at the scratch. In order to establish the location of the cathodic area as well as to determine the amount of Cu-replating around the filament, cyclic voltammetry utilizing a capillary electrode was performed on planar electrodes used in scribe-creep. Both charge transfer controlled and mass transport controlled cathodic reaction rates occurred at the fastest rates at the scratch and filament tail. The charge transfer controlled cathodic reaction rate was directly proportional to θ_{Cu} (surface coverage of Cu) while the mass transport limited rate was a complex nonlinear function of θ_{Cu}.[2] The material parameters controlling the anodic and cathodic reactions were thus elucidated. Control of the composition of the alloy as well as the size, number and distribution of the intermetallic particles controls the galvanic current when the cathodic current at the tail controls the galvanic corrosion process. However, when the galvanic corrosion process is anodically controlled, the content of Cu in solid solution was rationalized to be important through its influence on anodic reaction rates in acid solutions typical of the scribe creep head.

Finally, a galvanic couple model that describes scribe-creep rates in terms of the relevant processes at the tail (cathode) and head (anode) as well as ohmic voltage between the anode at the head and cathode at the tail was developed in order to explain the scribe-creep law of Equation [1]. As can be seen by Equation [2] the galvanic current is proportional to the galvanic potential, the ohmic resistance between the head and the tail, and the kinetic parameters governing the anodic and cathodic reaction rates. If the ohmic resistance between the head and tail increases then the galvanic current will decrease since ΔE is fixed. A panel with imbedded AA2024-T3 wires such as that shown by Figure 1 was utilized to measure the ORR kinetics as a function of distance from the scribe. The ohmic resistance (R_Ω) was also measured as a function of distance from the scribe. It was found that the R_Ω increased with distance from the scratch, l, with the relation l^n power. In the model, the relationship between R_Ω, l^n, and area is shown in Equation [3]. Equation [4] shows the relationship between the area of the scribe-creep, the scribe-creep length, $I_{galvanic}$, and the cathodic area. In this example, the galvanic current and, thus, the growth rate of the scribe-creep (dl/dt) is directly

affected by the area of the cathode and cathodic reaction rate (e.g., $I_{gal} = i_{cathode}A_{cathode}$). Thus $I_{galvanic}$ is a complex function of $i_{cathode}$, $A_{cathode}$, and l^n for cathodic controlled corrosion (Eq. [4]). By integrating Equation [4] it is easy to see the affect of time on the length of the scribe-creep (Equation [5]). At long times, the incremental change in the length of the scribe-creep becomes lower since 1/(n+1) is less than 1.

$$\Delta E_{galvanic} = E_{tail} - E_{head} = |\eta_{anodic}| + |\eta_{cathodic}| + I_{galvanic} R_{\Omega} \quad [2]$$

$$R_{\Omega} = \frac{\rho l^n}{A} \quad [3]$$

$$\frac{dA}{dt} \alpha\, w_{scribe} \frac{dl}{dt} \alpha\, I_{galvanic} \alpha\, f\left(\frac{i_{cathode} A_{cathode}}{l^n}\right) \quad [4]$$

$$l_{scribe} \alpha \left[\frac{(n+1) i_{cathode} A_{cathode}}{w_{scribe}}\right]^{(1/n+1)} t^{(1/n+1)} \quad [5]$$

Hence, the observation that scribe-creep obeyed an $l \alpha t^x$ relationship that could be explained by a galvanic corrosion model where $x \sim 1/n+1$. Figure 2 shows how increasing the area of the cathode would affect the galvanic current as expected in equation [5]. An increase in the galvanic current would in turn mean an increase in the scribe-creep growth rate as shown by Equation [4] of model. An increase in the galvanic current in turn means that the anodic corrosion rate must increase for a fixed anodic area. This galvanic corrosion model elucidates various ways to combat scribe-creep caused by under-paint corrosion. Scribe-creep can be combated by lowering i_{ca} by lowering i_o, A_{Cu}, and raising b_c. These alterations can be made by pretreatment or alloy design. The benefits of inhibitors that lower cathodic reaction rates or lower Cu replating provided another test of the model. Molybdate, cerium acetate and chromate were all found to lower scribe creep rates as expected by the model. The effect of alloying aging could also be explained by an anodically controlled variation of the model.

The scientific benefit is a better understanding of the factors that control scribe creep caused by underpaint corrosion on Al precipitation age hardened alloys. The technological benefit is that the exact impact of selected mitigation strategies can be clearly seen.

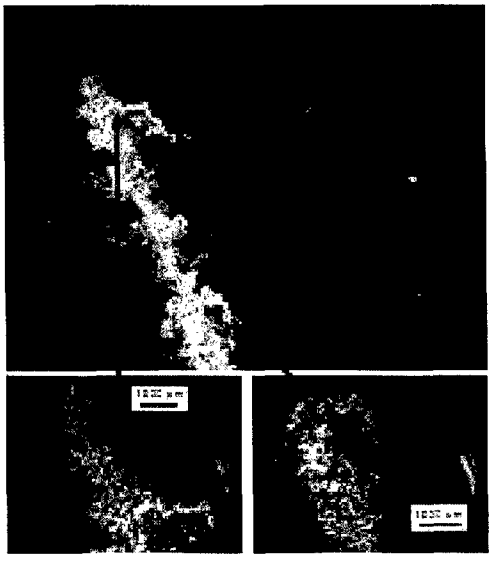

Figure 1. **Scribe-creep on an imbedded wire panel consisting of epoxy coated 2024-T3.**

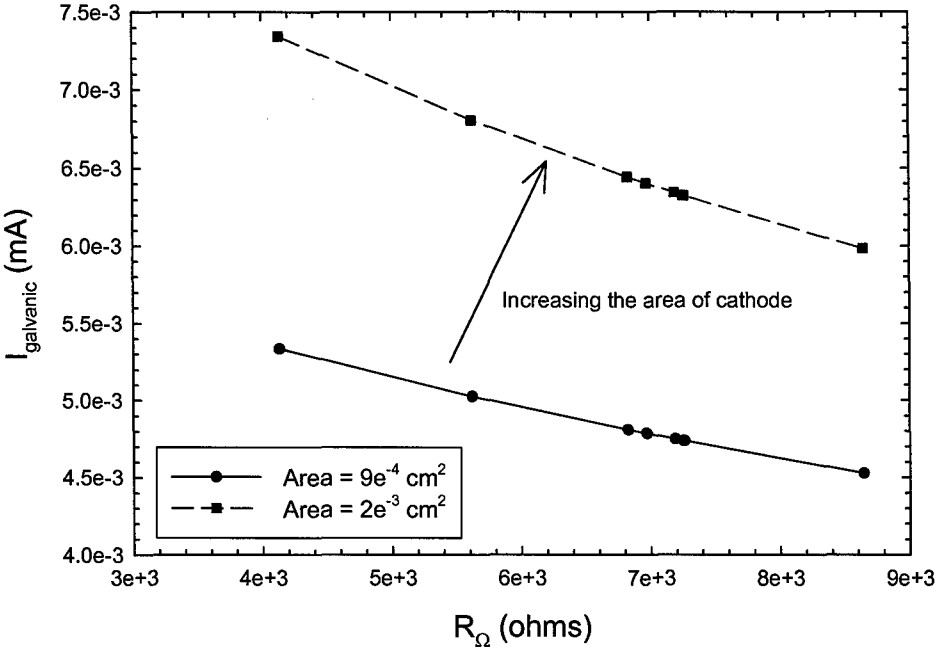

Figure 2. **Calculated galvanic current as a function of the measured ohmic resistance between unpretreated 115 μm diameter AA2024-T3 wires imbedded in a AA2024-T3 panel coated with an epoxy polyamide coating exposed to 80%RH at 40°C. Scribe creep rate decreases with increasing Ohmic resistance which increases with scribe creep length.**

1. H. Kaesche, Werkstoffe und Korrosion, vol. 11, p. 668-81, 1959.
2. M.A. Jakab, D.A. Little, and J.R. Scully, Journal of Electrochemical Society, vol. 152, p. B311-B20, 2005.

OBJECTIVE

The overall objective(s) of this study are to understand the role(s) of alloy composition, intermetallic phase density, identity and distribution and pretreatment on the global/overall initiation and propagation stages of under-paint corrosion that results in coating damage by scribe-creep away from a scratch in a painted surface that manifests itself as paint delamination. Specific goals include:

- Characterizing and understanding the role(s) of alloy composition, intermetallic compound (IMC) properties (e.g., anode, cathode, Cu replating source) as well as IMC density/spacing on the propagation of under-paint corrosion.

- Study the effects of pretreatments on under-paint corrosion through characterizing and understanding their effects on alloy surface alloy composition, intermetallic compound (IMC) modification (e.g., alteration of anode, cathode, Cu-replating source) in connection with the propagation stage of under-paint corrosion.

- Develop a model that links under-paint corrosion rate with key microstructure and pretreatment variables that govern this process.

Technical Goals

Our goals were to (a) apply spatially and temporally resolved methods to investigate the effects of alloy pretreatment and microstructural variables on under-paint corrosion initiation and propagation at intentional defect sites on aluminum aerospace alloys, and (b) perform global as well as high resolution measurements that enable both global and local processes associated with under-paint corrosion to be correlated with microstructural features and pretreatment effects on microstructural features (c) answer the questions proposed above concerning the role of microstructure in governing under-paint corrosion (d) develop a galvanic corrosion model to describe the scribe-creep growth process that accounts for effects of pretreatment and alloy microstructure.

REVISED STATEMENT OF WORK

The original project contained investigations on both organic coating defects and material heterogeneities. Upon the departure of S. Ray Taylor from UVA-CESE in 2003, the statement of work was revised to reflect those portions of the study continuing under Prof. John R. Scully. Those revised SOW are given below.

This revised study seeks to identify the origins of under-paint corrosion and the requisite environmental and material factors that promote under-paint corrosion propagation. Although the local chemical and electrochemical techniques used in prior research have increased our knowledge of under-film corrosion of aluminum alloys, many fundamental questions remain. These questions include (1) are defects sites that allow ion ingress through organic coatings the site of corrosion initiation regardless of the microstructural features located at such sites? and (2) what role does alloy composition, microstructure and intermetallic compounds (IMC) play in the initiation and propagation stages of under-film corrosion? This study will use experimental techniques devised in life sciences in conjunction with model alloys, spatially resolved electrochemical methods, and other novel substrate diagnostic techniques to precisely identify and delineate the roles of alloy composition, microstructure and IMCs in the origin of corrosion initiation and propagation of under-film corrosion. During the course of this project focus has been on the factors controlling the under-paint corrosion propagation. This will be achieved with the following revised tasks:

- Elucidation of the key microstructural parameters (e.g., alloy composition, intermetallic compound properties (anode, cathode, Cu replating source) and IMC density/spacing) that determine the risk of under-paint corrosion initiation and govern rates of propagation.
- Test the hypothesis that the types and (possibly the distribution) of IMCs exposed at local coating defects determine whether the site propagates or not.
- Characterize the transition from microgalvanic corrosion associated with IMCs on a micron scale to millimeter scale corrosion under paint.
- Determine whether the initial distribution of IMCs is important or whether Cu replating is the sole determining factor in the under-paint corrosion propagation and stifling stages

This revised statement of work supplants all previous statements and incorporates task modifications as per recommendations by Lt. Col. Paul Trulove through discussions in October-November 2003. The revised statement of work covers the periods from December 2003 to April 2005. Those listed below will continue for the duration of this grant activity. All personnel and task changes are reflected in an accompanying revised budget.

Project Technical Accomplishments

During the past year our technical progress has focused on performing high resolution measurements to measure local processes associated with under-paint corrosion that can be correlated with microstructural features, conducting global scribe-creep tests to characterized under-paint corrosion and subsequent paint delamination rates under various conditions, and

used microscopy to evaluate the affect of surface pretreatments on the microstructural features. A galvanic corrosion model to describe scribe-creep propagation as a function of substrate properties affected by these pretreatments was developed. The grand challenge was to identify changes in the surface composition and IMCs that would impact scribe-creep. Various material parameters that might control scribe-creep were elucidated.

Materials

Advanced methods of point pattern analysis were used to describe heterogeneous electrodes. Spatial analysis was performed on the AA2024-T3 unpretreated surface using L_2 statistics on the BSE images in order to determine if the IMCs are clustered or random in the material.

In addition, various model alloys were incorporated into this study. These included high purity Al, an Al-Cu binary alloy (Al-4.3Cu), an Al-Cu-Mg ternary alloy (Al-4.3Cu-1.3Mg), and various synthesized IMCs (Al_2Cu (θ-phase) and Al_2CuMg (S-phase)).

Technique Development

A standard reproducible method of producing scribe-creep was developed that can be sued for a number of Al alloys. A method involving cyclic voltammograms and regression analysis was perfected for determination of the extent of redeposited Cu present on AA2024-T3 surfaces after various pretreatments and aging treatments. This method was successfully extended to small specimen areas. In conjunction with post exposure paint stripping, this method is now being used to examine Cu-redeposition during under-paint corrosion. X-ray photoelectron spectroscopy (XPS) was used to correlate the amount of replated copper to the cyclic voltammetry results.

Cerium, Molybdenum, and Chromate pretreatments were utilized to compare the affect of other pretreatments on scribe-creep growth rate in comparison to the NaOH alkaline etch and the NaOH + HNO_3 pretreatments. . Drop-wise additions (periodic application of the inhibitor solutions) were also compared to the other pretreatments.

A capillary microprobe was developed in order to take localized measurements for mapping the replated Cu around a filament and distances from the original scratch (coating defect).

Specifically local electrochemical arrays were developed for use in under-paint corrosion. Localized electrochemical impedance tests were conducted during exposure in 80%RH at 40°C utilizing a AA2024-T3 panel with AA2024-T3 imbedded wires of 115 μm and 250 μm diameters.

Local and global measurements of scribe-creep rates promoted by under-paint corrosion

Tests were performed to investigate scribe-creep rates as a function of alloy aging and pretreatment on AA2024-T3 at various temperatures (25°C, 40°C, and 50°C). Analysis during testing was performed using optical microscopy and image analysis performed at various times during environmental exposure of the panels. For the coated panels of AA2024 exposed

to 80%RH at 25, 40 and 50°C, distinct differences in under-paint corrosion rate were seen for various treatments. Chiefly, treatments that lead to more significant replating of copper or that created a large capacity for copper replating lead to the worst scribe-creep indicative of more severe under-paint corrosion. Scribe-creep length increased with time to the ½ power and was thermally activated. Localized impedance spectroscopy was also performed on the panels at various distances away from the scribe utilizing the capillary electrode. Full immersion testing was conducted on coated AA2024 panels with various aging conditions which were scribed and exposed to a dilute HCl (pH ~ 2) solution showed rapid coating delamination and failure over a short period of time.

Electrochemical and Surface Science Measurements

Electrochemical and surface science testing to elucidate the role of surface pretreatment and alloy aging were conducted. The goal was to link surface condition (roughness and chemical) with under-paint corrosion rates. These included Cu replating characterization by cyclic voltammetry and x-ray photoelectron spectroscopy. Post-test analysis on scribe-creep panels included cyclic voltammograms, locally and globally, after coating removal to determine the change in replated copper due to the scribe-creep when compared to the unexposed panels. Utilizing the capillary microprobe localized measurements of the Cu-replating due to the scribe-creep process was mapped around a filament and distances from the scribe.

Galvanic Corrosion Model

A galvanic corrosion model has been constructed to explain the relationship between scribe-creep and metallurgical as well as pretreatment variables.

A galvanic couple exists between the anodic head and the cathodic tail of the scribe-creep filament formed during under-paint corrosion. The galvanic current results in anodic undercutting which is responsible for scribe-creep in Al alloys. The galvanic couple relationship is affected by the cathode area, cathodic kinetics per unit area, anodic kinetics, anode area and the distance between the head and tail as the filament grows. At the galvanic couple potential the sum of the anodic currents is equal to the sum of the cathodic currents over all areas (Equation [1]). This is always true, however, the local current densities are not always equal. Theoretically this means that if the area of the cathode (A_{Cu}) increases at constant cathodic kinetics per unit area, such as by Cu-replating, then the corrosion rate of the anode (i_a) or the anode area or both must increase to maintain the balance of Equation [1]. Therefore, the growth rate of scribe-creep should decrease as the area of the cathode decreases or as the cathodic kinetics per unit area are inhibited. Equation [2] states the basic fundamental equation for a galvanic couple which states that the difference in the mixed potentials of the anode and cathode is equal to the sum of the overpotentials plus the IR drop for the system.

$$\sum i_a A_a = \sum i_c A_c = I_{couple} \qquad [1]$$

$$\Delta E_{galvanic} = |\eta_a| + |\eta_c| + I_{galvanic} R_\Omega \qquad [2]$$

When the distance between the anodic head and cathodic tail increases that in turn increases the ohmic resistance of the galvanic couple. The galvanic current is decreased ($I_{galvanic} \downarrow$ as $R_\Omega \uparrow$) since ΔE is fixed and is given as the difference in open circuit potential between the anode and cathode (e.g., $\Delta E = E_{tail} - E_{head}$). Assuming that the rate of scribe-creep is proportional to the rate of galvanic corrosion, many of the pretreatment and metallurgical factors describing scribe-creep may be described within this framework.

In the case of scribe-creep by an anodic undercutting mechanism the growth rate of the scribe, dl/dt, is proportional to the galvanic current for the system as stated by Equation [3].

$$\left(\frac{dl}{dt}\right) \propto I_{couple} \qquad [3]$$

The total current density ($i_{cathode}$) is a function of the limiting and activation current densities for the cathodic reaction rate (*J.R. Scully, Advanced Electrochemistry, University of Virginia, 1999*) when under mixed control (Equation [4]). Assuming that the galvanic couple current is controlled by total cathodic current then the growth rate of scribe-creep area (l is the scribe-creep damage length and w is the width of the scribe area) is proportional to the total cathodic reaction rate (Equation [5]). The scribe-creep area growth rate is then a function of $i_{cathode}A_{cathode}$ and is inversely proportional to the distance from the anode at the head and the cathode at the tail raised to some power n accounting for non-linearity (l^n) in the R_Ω vs. l relationship as shown by Equation [5]. The scribe-creep length is seen to be a function of the cathodic reaction rate and θ_{Cu}, or the surface coverage of copper. Rearranging (Equations [6]-[7]) it is observed that the length is directly proportional to $t^{1/n+1}$ (Equation [8]). It can also be seen how either a $t^{1/2}$ or deviation from $t^{1/2}$ growth law can occur.

$$i_{cathode} = \left(\frac{i_L \times i_{act}}{i_L + i_{act}}\right)_{ORR} + i_{HER} \qquad [4]$$

$$\frac{dA}{dt} = w_{scribe}\frac{dl}{dt} \;\alpha\; I_{couple} \;\alpha\; \frac{i_{cathode}A_{cathode}}{l^n_{scribe}} \qquad [5]$$

$$l^n_{scribe}\,dl \;\alpha\; \frac{i_{cathode}A_{cathode}}{w_{scribe}}\,dt \qquad [6]$$

$$\frac{l^{n+1}_{scribe}}{n+1} \;\alpha\; \frac{i_{cathode}A_{cathode}\,t}{w_{scribe}} \qquad [7]$$

$$l_{scribe} \;\alpha\; \left[\frac{(n+1)\,i_{cathode}A_{cathode}}{w_{scribe}}\right]^{(1/n+1)} t^{(1/n+1)} \qquad [8]$$

From these equations it should be possible to predict the growth rate for the filaments or under-paint corrosion. It should also be possible to anticipate what metallurgical, pretreatment or inhibitor factors could impact scribe-creep. It can also be seen how improved adhesion might help because in the case of better adhesion a given increase in the right hand side of Eq. 8 would produce less increase in l_{scribe}. Scribe length would increase less for a given value of $i_{cathode}$ $A_{cathode}$. Therefore, the dependency of the length of under-paint corrosion after a given time period can be linked to factors (i.e, $i_{cathode}$, $A_{cathode}$) that can be controlled through the use of surface pretreatments and inhibitors.

The open circuit potentials for unpretreated AA2024-T3, NaOH pretreated AA2024-T3, and pure Cu were measured and inserted into Equation [2] for E_{tail}. The value for E_{head} was determined from anodic potentiodynamic scans performed on unpretreated AA2024-T3. Coupled with the increase in R_{Ω} as the distance from the head to tail increased, the drop in $I_{galvanic}$ and $i_{cathode}$ can be computed. Thus at long scribe lengths growth occurs at a slower rate.

III. Accomplishments and New Findings

Results from scribe-creep testing (under-paint corrosion from a scribe paint defect) of AA2024-T3 under selected constant humidity levels and various temperatures indicated distinct differences in steady state under-paint corrosion and delamination rates as a function of temperature, redeposited Cu content and presence of copper-bearing IMCs. Specifically:

- Scribe-creep rates on coated AA2024-T3 after all pretreatments were faster than observed on high purity Al and were accelerated by temperature.
- There is a clear relationship between scribe-creep growth rate and length and pretreatments that replate copper or provide a large capacity for Cu replating. However, all pretreatments experienced acceleration of scribe-creep length with temperature.
- To first approximation, scribe-creep follows Arrhenius growth rate behavior.
- Scribe-creep growth decreased with time in a complex manner that is best described as $t^{(1/n+1)}$ where $n>1$.
- Coated AA2024-T3 with large amounts of replated Cu and/or large capacity for replating Cu, exhibited the largest increases in scribe-creep rate with temperature. Scribe-creep rates could be predicted based on prior Cu redeposition and the propensity for Cu redeposition.
- Chemical surface pretreatments which preferentially remove copper and copper sources (IMCs) for replating from the surface improve scribe-creep resistance. However, scanning electron microscopy (SEM) showed that the NaOH etch followed by immersion in the HNO_3 deoxidizer pretreatment did not removal all the sources of copper.
- Similarly, inhibitors that suppress Cu-replating and inhibit ORR lower $i_{cathode}$ $A_{cathode}$ to reduce scribe-creep.

Electrochemical and surface science testing to elucidate the role of surface pretreatment, inhibitors and heat treatment on scribe-creep rates have found that:

- Cyclic voltammetry indicated that exposure to NaCl solutions and NaOH pretreatment significantly increased redeposited Cu on bare surfaces of AA2024-T3. Cathodic E-log I confirmed enhancement of both charge transfer controlled and mass transport controlled ORR with Cu-replating.
- Cyclic voltammetric tests indicated that the NaOH + HNO_3 pretreatment produced a surface that exhibited low levels of Cu redeposition and resisted further redeposition during scribe-creep tests on coated AA2024-T3.
- Cyclic voltammetry tests performed on the other two cleaning procedures indicated that both the Brulin pretreatment (immersed for 5 min in a 10% Brulin 815GD solution, tap water rinse, immersion in an alcoholic phosphoric acid deoxidizer for 2 min, and finally a DI water rinse) and the HNO_3 + HF pretreatment (1 min immersion in a 50% (vol) HNO_3 + 2% (vol) HF solution at room temperature, immersion in a 2.5% NaOH alkaline solution at 35-40°C for 1 min, and finally immersion in a 50% (vol) HNO_3 + 2% (vol) HF solution for 1 min with a DI water rinse between each step) were more efficient at removing the sources for copper replating than the 40 min alkaline etch in 1.5 g/L NaOH followed by 30 sec in HNO_3 pretreatment. This will be confirmed using SEM.
- Scribe-creep tests were performed on as-received, NaOH + HNO_3 pretreated, and Cerium, Molydenum, and Chromate inhibitor pretreatments and drop-wise tests. The results showed that the scribe-creep growth rate on the NaOH + HNO_3 pretreated AA2024-T3 was similar to the inhibitor pretreatments. The inhibitor drop-wise panels had a scribe-creep growth rate similar to or worse than the as-received condition. These results
- The galvanic corrosion model for scribe creep propagation was developed that was useful to understand the factors governing scribe creep propagation during underpaint corrosion of precipitation age hardened Al alloys.
- The galvanic corrosion model was used in simulations to help elucidate the impact of alloying, heat treatment, surface pretreatment and inhibitors than alter interfacial kinetics when simplifications were made regarding the role(s) of these factors on scribe creep.

IV. Personnel Supported

J.R. Scully	PI (U. of Virginia)	5% effort
Daryl Little	Ph.D. candidate	100% effort
Geoff Biddick	Undergraduate researcher	50% effort
Francisco Presuel	Post-doctoral researcher	20% effort

V. Interactions/Transitions

Participation at Professional Meetings, Conferences and Seminars

- John. R. Scully, was Chairman of the Gordon Research Conference on Aqueous Corrosion, held July 25-30, 2004 New London, New Hampshire.

- D.A. Little, J. Ferrell, and J.R. Scully, "The Influence of Surface Cu-content on the Under-paint Corrosion of Aluminum Alloy AA2024-T3", in CORROSION/2004, in Advances and Future Directions in Military Coating Systems (STG 40), NACE March 28 – April 1 in New Orleans, LA (2004).

Consultive and Advisory Activities

- Consultant to Dr. Jill Illett (S&KT Technologies), Deb Peeler (WPAFB) on "Characterizing Coating Degradation and Corrosion of Organically Coated Aluminum Aerospace Alloys SBIR contract F33615-02-C-5619 (award date 25 September 2002). Consulting effort includes review of coating test plans and test results, as well as consultation regarding equivalent circuit modeling of organic coating/metal interfaces.

- Consultant to the Columbia Accident Investigation Board (CAIB) regarding corrosion issues associated with the Orbiter Columbia and the remaining Orbiter Fleet. Task 1 concerns the effects of a Thermal Protection System (Tile) repair practice that omits Koropon Chromate Primer in reinstallation. The issue concerns whether there will be corrosion and loss of tile adhesion as a consequence of this omission.

- Consultant to the Columbia Accident Investigation Board (CAIB) regarding corrosion issues associated with the Orbiter Columbia and the remaining Orbiter Fleet. Task 2 concerns whether there are foreseeable modes of long-term corrosion degradation that can affect the thermal protection system if orbiter corrosion is inspected but not repaired.

- Consultant to Dr. M. Inman (Faraday Technologies), Deb Peeler (WPAFB) on SBIR project titled "Forecasting the Coating Breakdown and Corrosion of Organically Coated Aluminum Aerospace Alloys," Faraday Technologies, Dayton, Ohio. Consulting effort includes review of coating test plans and test results, accelerated lab test environments as well as consultation regarding equivalent circuit modeling of organic coating/metal interfaces.

- Consultant to Apple Computer regarding Al anodizing of Apple Powerbooks.

Transitions - Professional Communications (include date, persons involved, objective, contact information)

- Dr. Dave Barrington
  UDRI Materials Engineering Division
  Coatings Group Leader

UDRI/CTIO Program Manager
300 College Park
Dayton, OH 45469
Dates: November 18th, 2004, April 15th, 2005
Objective: Guidance on another pretreatment procedure used by AF.

- Dr. Tony Hughes
  Professorial Fellow, RMIT University
  Team Leader Corrosion Science & Surface Design
  CSIRO Manufacturing & Infrastructure Technology
  Gate 4, Normanby Road
  Clayton, Victoria 3168, Australia
  Dates: various dates
  Objective: Pretreatment procedure and corrosion product removal procedure used by Australia.

- Dr. Alison Davenport
  School of Engineering
  Metallurgy and Materials
  The University of Birmingham
  Edgbaston
  Birmingham B15 2TT, UK
  Dates: various dates
  Objective: Guidance on cyclic voltammetry procedure, surface pretreatment procedure, and surface microstructure associated with Cu-containing Al-alloys.

- Dr. C Jeffrey Brinker
  Professor: Chemical Nuclear Engineering
  University of New Mexico
  1001 University Blvd SE Rm 209
  Albuquerque, NM 87131
  Dates: August 2, 2004, May 23-25, 2005
  Objective: Supplier of Cerium powders for coatings and pretreatments.

- Dr. William Smyrl
  Professor
  Department of Chemical Engineering and Materials Science
  University of Minnesota at Minneapolis St. Paul
  151 Amundson Hall
  421 Washington Ave. SE
  Minneapolis, MN 55455
  Dates: August 2 – present 2004
  Objective: Guidance on corrosion product removal procedure.

- Dr. M. Inman
  Senior Engineer

Faraday Technologies,
Dayton, Ohio 45409
Dates: various dates, April 2005
Objective: Supplier of AA2024-T3 with mil spec surface preparation and mil-spec coating for comparison studies of degradation of a polyamide-cured bisphenol A-based epoxy coating similar to aircraft primers. Providing guidance to her on EIS testing circuit models to describe the coating / metal interface.

Publications and Presentations

a. Referred Journals

- N.D. Budiansky, F. Bocher, H. Cong, M.F. Hurley, D.A. Little, J.R. Scully, "Use of Coupled Multi-Electrodes to Advance the Understanding of Selected Corrosion Phenomena," Corrosion Journal, in preparation August (2005).

- D.A. Little, M.A. Jakab, and J.R. Scully, "The Effect of Pretreatment on the Under-Paint Corrosion of AA2024-T3 at Various Temperatures," Corrosion Journal, Accepted – in press, June (2005).

- M.A. Jakab, D.A. Little, and J.R. Scully, Experimental and Modeling Studies of the Oxygen Reduction Reaction on AA2024-T3, Journal of Electrochemical Society, vol. 152, p. B311-B20, 2005.

- D.A. Little, B.J. Connolly, and J.R. Scully, "An Electrochemical Framework to Explain the Intergranular Stress Corrosion Path in Two Al-Cu-Mg-Ag Alloys," Corrosion Science, Submitted, December (2004).

- G.O. Ilevbare, O. Schneider, R.G. Kelly, J.R. Scully, "In-situ Confocal Laser Scanning Microscopy of AA2024-T3 Corrosion Metrology: Part 1. Localized Corrosion of Constituent Particles," J. Electrochem. Soc., vol 151, pp B453-B464, 2004.

- O. Schneider, G.O. Ilevbare, J.R. Scully, R.G. Kelly, "In-situ Confocal Laser Scanning Microscopy of AA2024-T3 Surface Corrosion Metrology: Part 2. Trench Formation around Particles," J. Electrochem. Soc., vol 151, pp B465-B472, 2004.

- Brian J. Connolly, J.R. Scully, "An Electrochemical Framework for Intergranular SCC Susceptibility as a Function of Isothermal Aging Time for an Al-Li-Cu-X Alloy," Corrosion Journal, in preparation September (2003).

- Brian J. Connolly, J.R. Scully, "The Transition from Localized Corrosion to SCC in a Severely Underaged Temper of Al-Li-Cu-Ag Alloy AA 2096," Corrosion Journal, Accepted, In Press, May (2005).

b. Books/Book chapters/Books edited

Books

- none.

Books Edited

- Section Editor: ASM Metals Handbook, Vol. 13, **Section on Fundamental Corrosion Processes**. ASM, Metals Park, OH, pp. 42-86, (2004).

- Section Editor: Section on *Forms of Corrosion*, **ASTM Manual 20 on Corrosion Tests and Standards**, Version II, ASTM Philadelphia, PA., pp. 204-340, (2005).

Book Chapters Written

- J.R. Scully, Chapter on **Electrochemical Methods in Laboratory Corrosion Testing**, in **ASTM *Manual on Corrosion Tests and Standards, Application and Interpretation 2nd ed.***, ASTM West Conshohoken, PA, pp. 107-130, (2005).

- J.R. Scully, R.G. Kelly, Chapter on **Electrochemical Methods in Laboratory Corrosion Testing**, in ASM Metals Handbook, Vol. 13A, CORROSION, Fundamental, Testing and Protection, pp. 68-80, ASM, Metals Park OH (2003).

c. Proceedings

- D.A. Little, J. Ferrell and J.R. Scully, "The Role(s) of Substrate Alloy Heterogeneity and Composition In the Under-paint Corrosion of Cu-bearing Al Alloys, "Tri-Service Corrosion Conference, Las Vegas, NV, Nov. (2003).

- D.A. Little, J. Ferrell and J.R. Scully, The Influence of Surface Cu-content on the Under-paint Corrosion of Aluminum Alloy AA2024-T3, NACE CORROSION/04 Conf., New Orleans, LA, Paper no. 04277, March, (2004).

- D.A. Little, J.R. Scully, "Use of Coupled Multi-Electrodes to Elucidate Controlling Factors in Corrosion-Induce Scribe Creep on AA 2024-T3," Tri-Service Conference on Corrosion, Orlando, November 05, in preparation August (2005).

- N.D. Budiansky, F. Bocher, H. Cong, M.F. Hurley, D.A. Little, J.R. Scully, "Use of Coupled Multi-Electrodes to Advance the Understanding of Selected Corrosion Phenomena," Corrosion Journal, in preparation August (2005).

Awards and Honors

John R. Scully, Francis L. LaQue Award of ASTM, 2005.

John R. Scully, Fellow of the Electrochemical Society, 2005.

John. R. Scully, Chaired the Gordon Research Conference on Aqueous Corrosion, July 25-30, 2004 New London, New Hampshire

D.A. Little, Harvey Herro Award for best posters in Applied Corrosion Technology – 1st Place: CORROSION/2004. NACE, New Orleans, LA, March 2004.

Appendix

Effect of Surface Pretreatment, Temperature, and Aging on Cu-replating and Scribe-Creep

- D.A. Little, J. Ferrell and J.R. Scully, The Role(s) of Substrate Alloy Heterogeneity and Composition In the Under-paint Corrosion of Cu-bearing Al Alloys, Tri-Service, Las Vegas, NV, Nov. 2003.

- D.A. Little, J. Ferrell and J.R. Scully, The Influence of Surface Cu-content on the Under-paint Corrosion of Aluminum Alloy AA2024-T3, NACE, New Orleans, LA, Paper no. 04277, March, 2004.

- D.A. Little, M.A. Jakab, and J.R. Scully, "The Effect of Pretreatment on the Under-Paint Corrosion of AA2024-T3 at Various Temperatures," Corrosion Journal, Submitted and Reviewed, June (2005).

Localized Cu-replating Measurements to Establish the Location of the Cathodic Area

Large scale or global measurements of Cu previously performed on post coating removal coupons have revealed an overall replated Cu concentration equal to or lower than the pre-exposure cyclic voltammograms, possibly due to a tenacious corrosion product on the surface. In order to quantify the localized Cu-replating along the various regions of a filament, cyclic voltammograms will be performed utilizing a capillary microprobe, which is illustrated in Figure 1. The measurements of Cu-replating using the capillary at various locations from the original scribe to the tip of the filament and in front of the filament were performed to determine the main cathodic area. A tip diameter of ~250 μm was used which will made the tip diameter approximately the same size as the width of the filament heads. The SEM images in Figure 2 show the size of the tip on the surface of the sample. The tip size is equal to the area inside the red circle. A Femtostat® (Gamry) was used due its capability of measuring low currents and offered high current resolution and lower noise levels.

a)

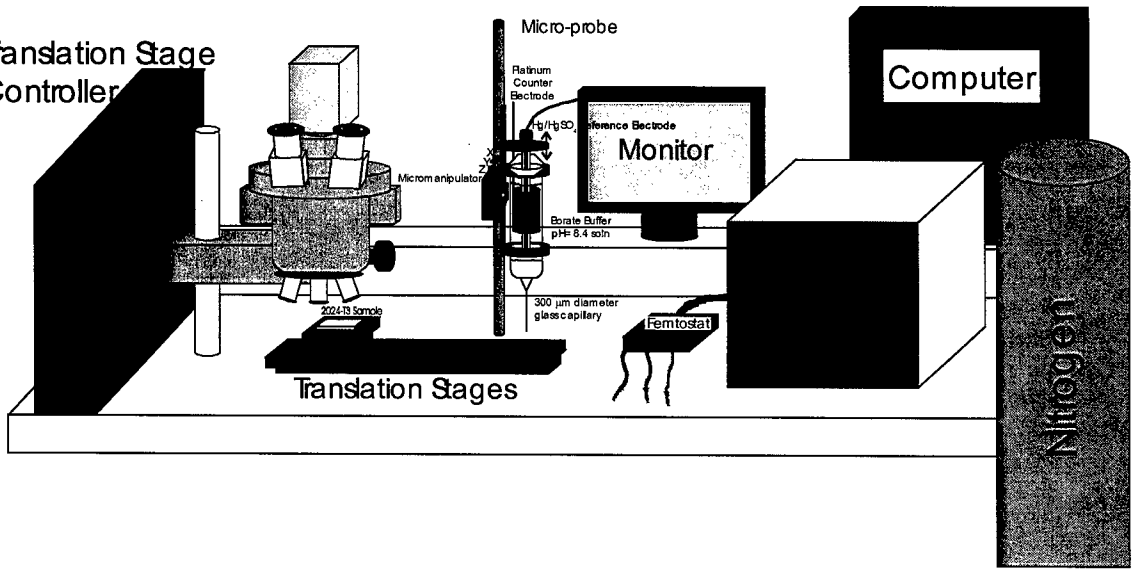

b)

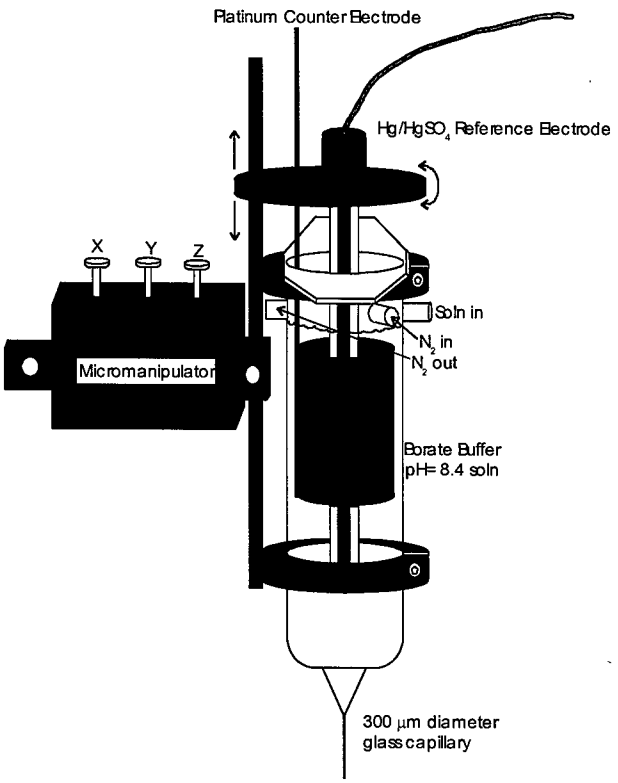

Figure 1. **The Electrochemical Capillary Micro-Probe (ECM) setup is shown in a), including the Faraday cage and nitrogen tank. A blowup of the ECM cell is shown in b).**

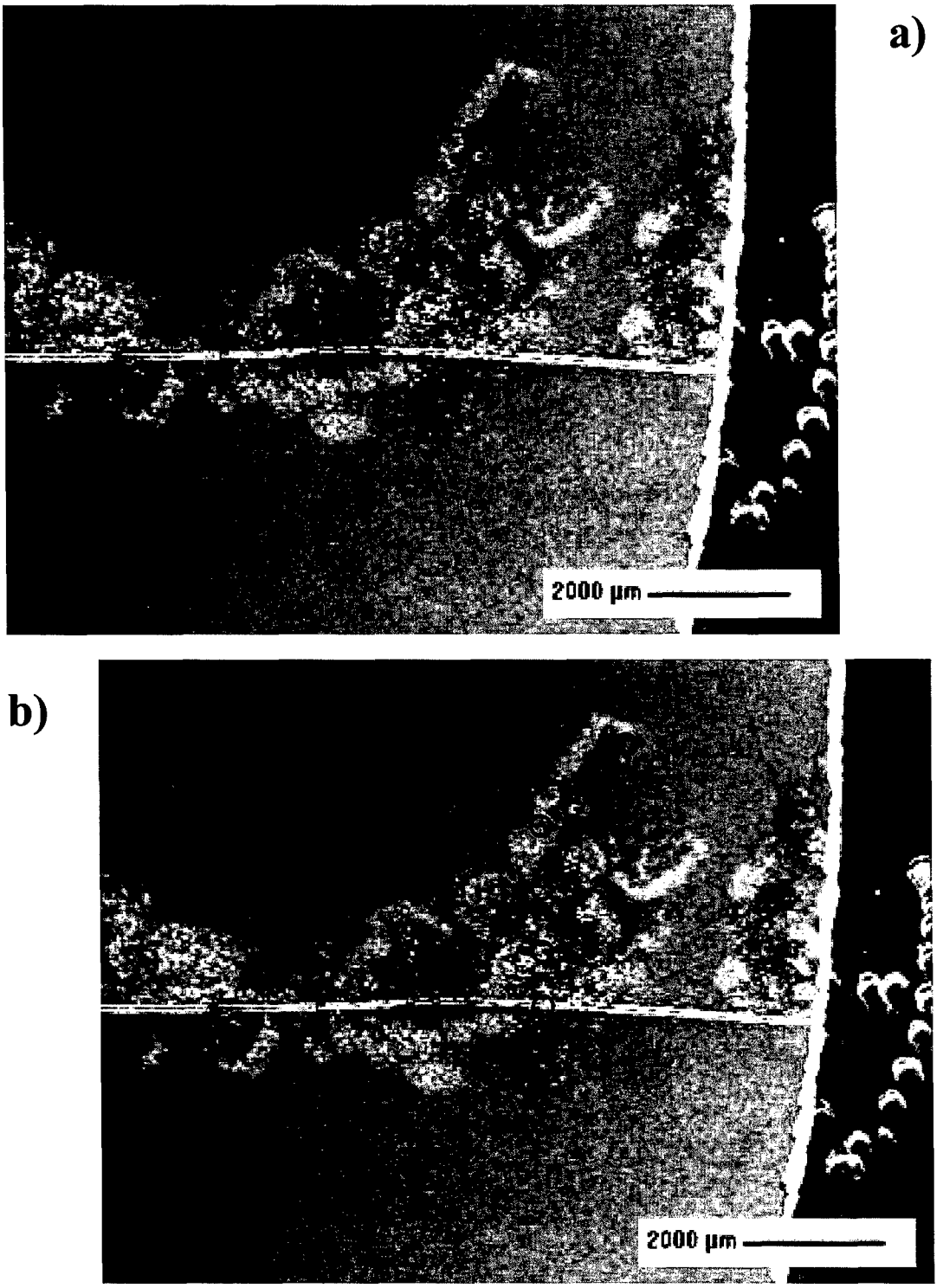

Figure 2. **SEM micrographs of unpretreated AA2024-T3 post humidity exposure and coating removal. a) and b) are the same area but used for comparison purposes. The red circles represent the size diameter of the capillary electrode (300 µm) and indicate the possible spatial resolution.**

The basic setup of the cell used for these tests is shown in Figure 1b. The cell consists of a cell body with inlets for the N_2 and solution and an outlet for the air. Contained in the cell body is an $Hg/HgSO_4$ reference electrode surrounded by a platinum coated niobium mesh counter electrode. These tests were performed in deaerated Borate Buffer (pH=8.4) using the same procedure that was utilized for the large scale CV tests. The tip of the cell is a glass capillary pulled to small diameters.

Borosilicate glass capillary tubing with an inside diameter of approximately 710 μm and a wall thickness of about 175 μm was pulled. This yielded a tip size of approximately 5-7 μm in diameter. The tips of the glass capillaries were then polished flat to a given diameter using a heavy steel body on a water film on rotating 1200 grit SiC grinding paper. An example of a tip with a diameter of ~84 μm is shown by the micrographs in Figure 3. After the tip is polished flat the glass is secured to a syringe tip (Figure 3b). A silicone seal is applied to the tip in order to achieve a good seal and prevent solution leakage. Suter[1] showed that the seal applied to the tip of the capillary must be thick in order to have reproducible results. The ideal thickness determined by Suter[1] is about half the tip diameter and this is achieved by coating the tip using several cycles. The tip is dipped into a cold hardening silicone rubber (Dow Corning® 3140). The capillary is then flushed with ethanol to remove the silicone rubber in the tip. The silicone is then smoothed before reapplication of the silicone rubber. Liquid soap on an acrylic surface prevents the silicone from sticking during the smoothing process. Finally the capillary is dipped into ethanol to remove the soap. The tip is then screwed onto the end of the cell body which is deaerated with N_2 and filled with deaerated borate buffer pH=8.4 solution.

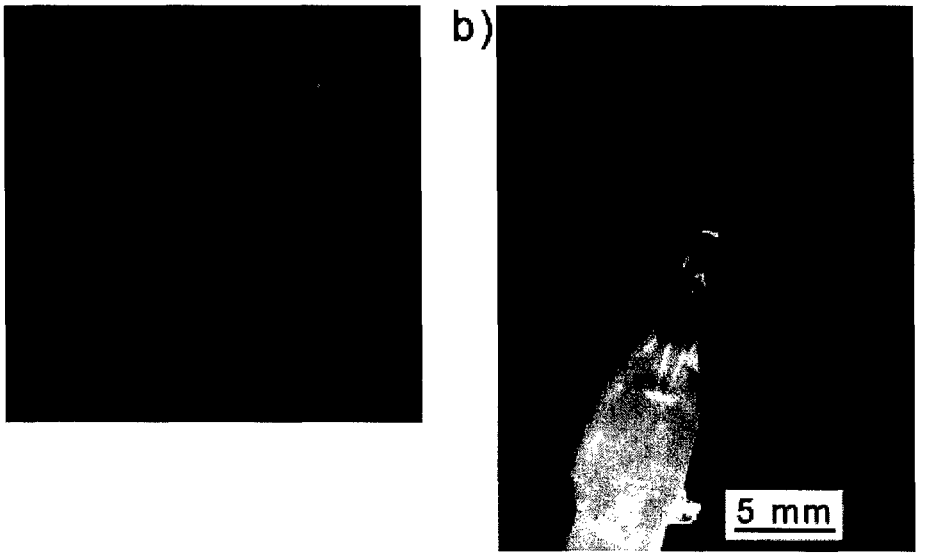

Figure 3. **Glass capillary tip used for ECM. a) shows the diameter of the tip and b) shows the whole capillary tip.**

An Olympus® BXFM microscope mounted on a boom stand is used to identify the area of interest to be tested. The sample is then translated on Newport® (M-)ILS X-Y linear stages, which were also utilized for moving the sample to the area of interest, to the capillary electrode.

The capillary cyclic voltammetry experiments were performed on unpretreated and NaOH + HNO_3 pretreated AA2024-T3. However, due to the low currents a scan rate of 10 mV/sec was used. Figure 4 shows that for the smaller scale areas faster scan rates produce larger peak heights. However, at 20 mV/sec the instrument has a problem with the auto-ranging and results in current spikes.

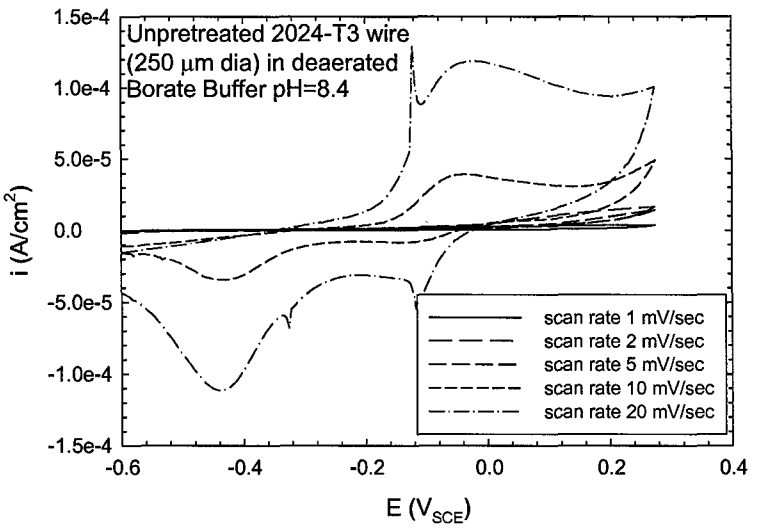

Figure 4. **Effect of scan rate on the Cu peak height for unpretreated AA2024-T3 in deaerated borate buffer (pH=8.4).**

Establishing the Role of Cu-Replating on ORR Kinetics

In order to measure the ohmic resistance as a function of the distance from the scratch as well as when the scribe-creep reaches given distances from the scratch, panels with wires imbedded in them were designed. A back plate was designed to attach to the back of a 50 mm x 50 mm AA2024-T3 sheet in order to protect the wires as well as to supply stability to the 0.29 mm thick sheet. A schematic of the back plate is shown in Figure 5. The coupon was drilled with holes for the wires to be fed through. A schematic of the hole pattern is shown in Figure 6.

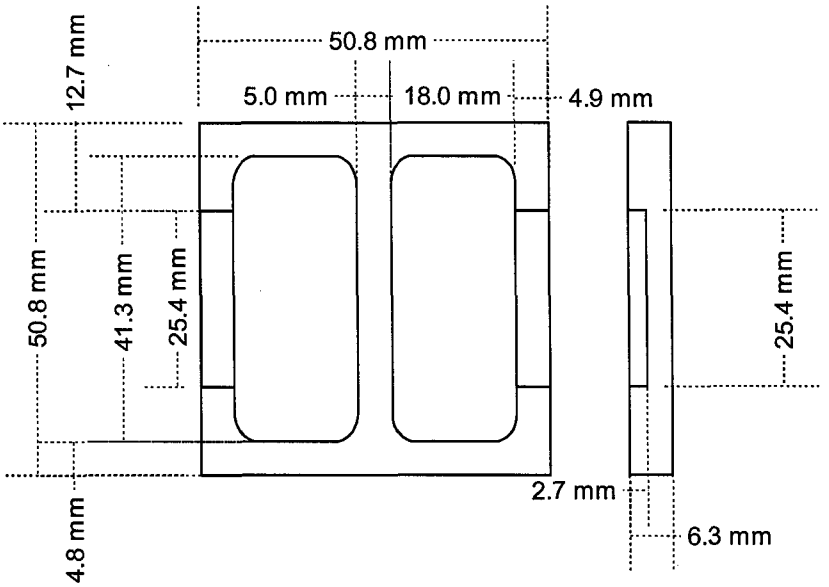

Figure 5. **Schematic diagram of back plate used for imbedded wire panels.**

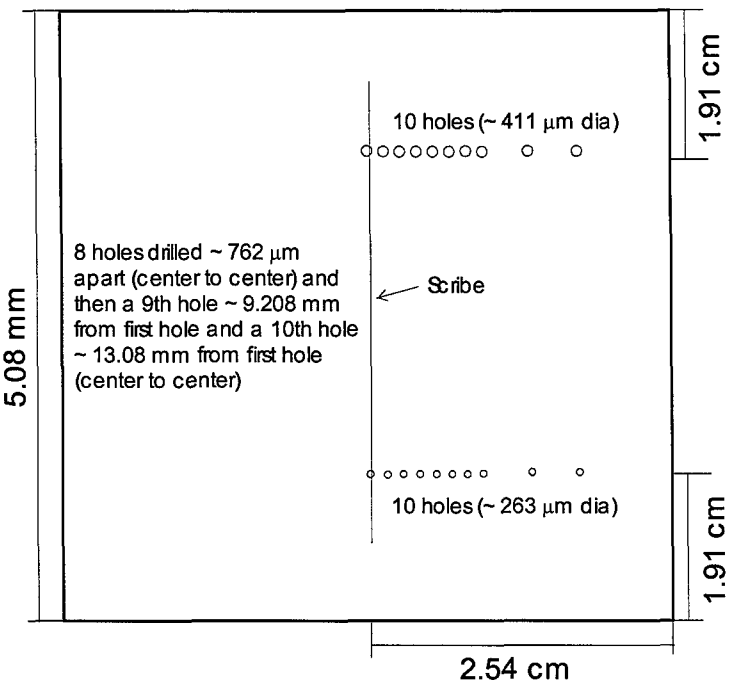

Figure 6. **Schematic diagram of hole pattern drilled into 0.29 mm thick sheet used for imbedded wire panels.**

Polyimide coated AA2024 wires of 115 μm and 250 μm diameters were attached to the sockets by stripping the coating from the ends, dipping them into a conductive epoxy, and pushing them into the receptive side of the plugs as shown in Figure 7a. Mill-Max® single in-line strip sockets with a standard solder tail were used for the socket plugs. After the holes were drilled in the coupon as shown in Figure 7b the other end of the wire was fed through these holes as can be seen in Figure 7c. During the course of the assembly the wires were

tested for conductivity between the pin on the socket and the end of the wire. They were also tested to ensure there are no shorts between pins and between the wires and the sheet. The sockets were then glued to a back plate (Figure 7d and e) and then this back plate was glued to the sheet yielding the product shown in Figure 7f-h. The back plate was then filled with epoxy to hold the wires in place. These panels were then prepped in the same manner as the scribe-creep panels. The panels were ground to 1200 grit then coated, cured, scratched through the back row of wires as was shown in the schematic diagram in Figure 6, HCl initiated, and exposed at 40°C in 80%RH.

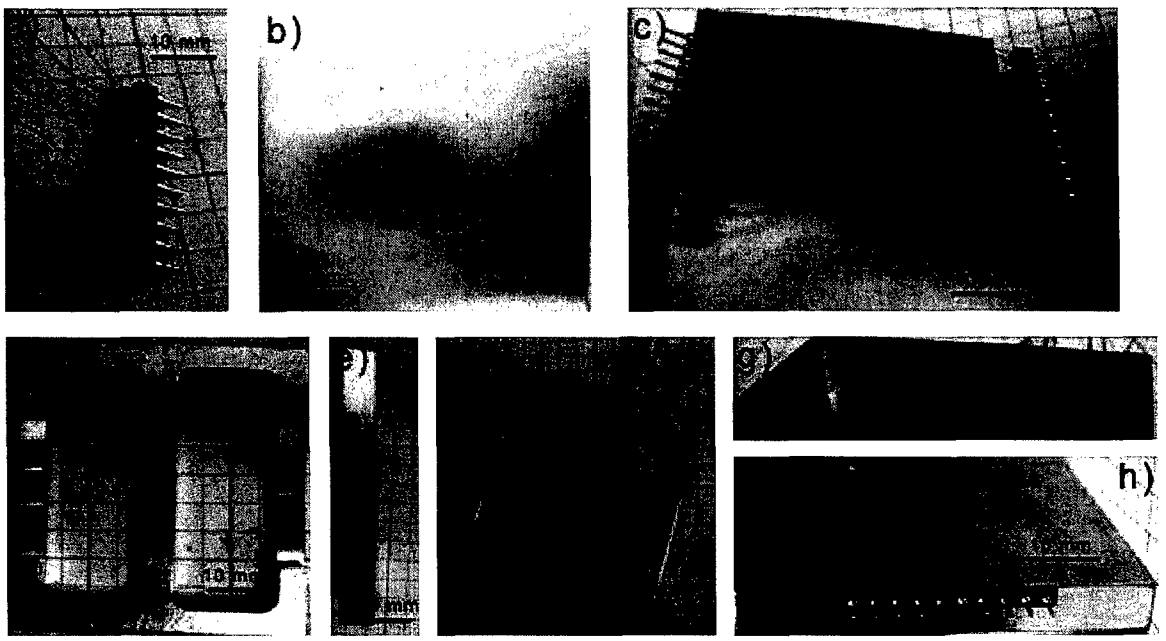

Figure 7. **Imbedded wire panel assembly steps. a) shows the sockets used, b) the panels sheet with holes drilled, c) wire fed through the hole, d) and e) the back plate, f),g) and h) the complete assembly.**

The panels were removed periodically during the exposure period in order to measure the impedance between the wires and to take digital micrographs of the scribe-creep growth. Using the scratched wires as both the counter electrode and the reference electrode a two electrode impedance measurement was performed between the wires using the coating as the moist coating as the electrolyte. For example wire 1 (the wire in which the scratch went across) was tested against wire 2, then wire 1 vs. wire 3, then wire 1 vs. wire 4, and etc. The impedance measurements were performed on a Princeton Applied Research Parstat 2263® using PowerSINE 2.4 software in the PowerSuite™ 2.55 software package. The frequency was swept from 10^6 Hz to 10^{-2} Hz.

References

1. Suter, T.A., *Mikroelektrochemische Untersuchungen bei austenitischen <<rostfreien>> Stählen: Messtechnik - Lochinitiierung - Mikroelektrochemie an Schweissnähten*, in *Technischen Wissenschaften*. 1997 (Dissertation), Eidgenössischen Technischen Hochschule Zürich: Zürich.